Physica A 493 (2018) 54–68

Contents lists available at ScienceDirect

Physica A

journal homepage: www.elsevier.com/locate/physa

Multi-channels coupling-induced pattern transition in a tri-layer neuronal network

Fuqiang Wu [a], Ya Wang [a], Jun Ma [a,d,*], Wuyin Jin [b], Aatef Hobiny [c]

[a] Department of Physics, Lanzhou University of Technology, Lanzhou 730050, China
[b] College of Mechano-Electronic Engineering, Lanzhou University of Technology, Lanzhou 730050, China
[c] NAAM-Research Group, Department of Mathematics, Faculty of Science, King Abdulaziz University, Saudi Arabia
[d] College of Electrical and Information Engineering, Lanzhou University of Technology, Lanzhou 730050, China

HIGHLIGHTS

- Pattern synchronization is investigated within a three-layer network.
- Diffusive collapse in parameter can induce pattern transition.
- Synchronization approach is dependent on the channel number connected two layers.
- More coupling channels can enhance the pattern synchronization.

ARTICLE INFO

Article history:
Received 2 July 2017
Received in revised form 24 September 2017
Available online 3 November 2017

Keywords:
Neuronal network
Collapse
Target wave
Pattern formation

ABSTRACT

Neurons in nerve system show complex electrical behaviors due to complex connection types and diversity in excitability. A tri-layer network is constructed to investigate the signal propagation and pattern formation by selecting different coupling channels between layers. Each layer is set as different states, and the local kinetics is described by Hindmarsh–Rose neuron model. By changing the number of coupling channels between layers and the state of the first layer, the collective behaviors of each layer and synchronization pattern of network are investigated. A statistical factor of synchronization on each layer is calculated. It is found that quiescent state in the second layer can be excited and disordered state in the third layer is suppressed when the first layer is controlled by a pacemaker, and the developed state is dependent on the number of coupling channels. Furthermore, the collapse in the first layer can cause breakdown of other layers in the network, and the mechanism is that disordered state in the third layer is enhanced when sampled signals from the collapsed layer can impose continuous disturbance on the next layer.

1. Introduction

The mammalian brain is composed of a large number of neurons and these neurons can present various firing patterns and dynamical properties in electrical activities by applying appropriate external stimulus. Since the breakthrough in electrophysiology achieved by Hodgkin and Huxely, the biological neuronal model [1] based on neuraxon of squid and its improved versions [2–6] have been used to investigate the dynamical properties of isolate neuron, collective behaviors of neurons, pattern selection and synchronization of networks. For example, *Volman et al.* [7] proposed a neuron–astrocyte model to detect the effect of astrocyte on neuronal activities. *Gu et al.*, [8] discussed the bifurcation behavior based on

* Corresponding author at: Department of Physics, Lanzhou University of Technology, Lanzhou 730050, China.
E-mail address: hyperchaos@163.com (J. Ma).

https://doi.org/10.1016/j.physa.2017.10.041
0378-4371/

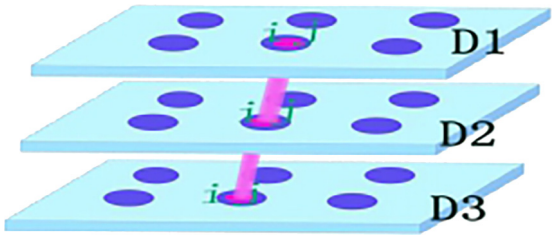

Fig. 1. Schematic diagram for a tri-layer network. Blue dollar spot represents neuron on each layer, and purple tube marks the coupling channel between layers. D1 is first layer, D2, D3 is the second, third layer of the network. (For interpretation of the references to color in this figure legend, the reader is referred to the web version of this article.)

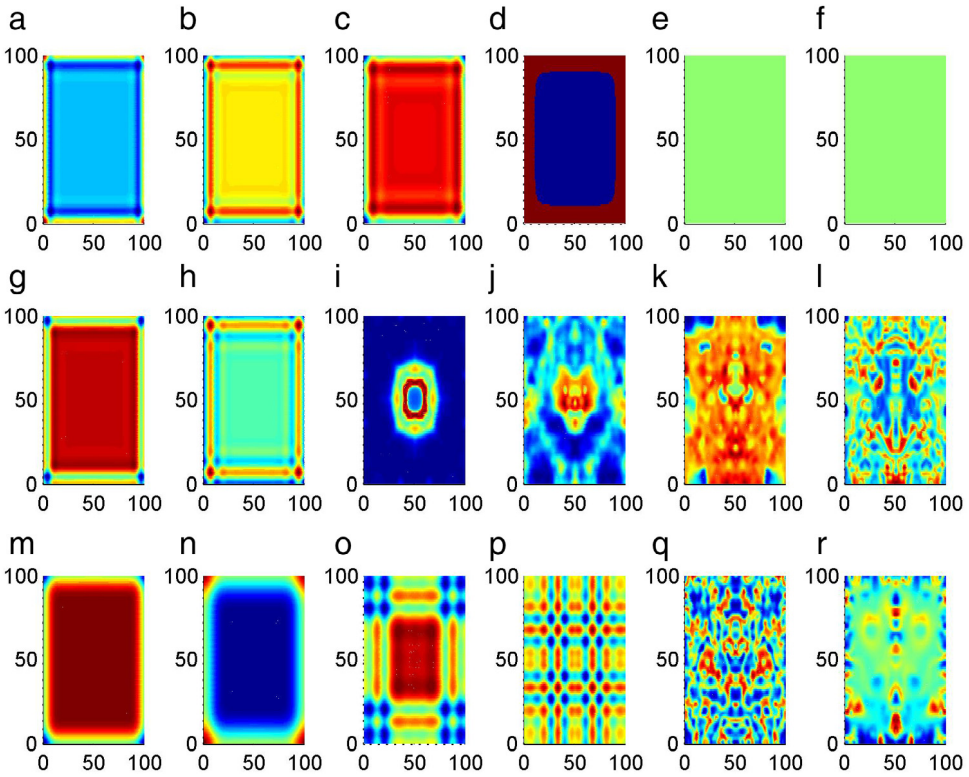

Fig. 2. Developed spatial pattern is plotted for the tri-layer network at $t = 50, 150, 500, 1000, 1500, 2500$ time units. The first layer (a)–(f) is driven by $I_{1ext} = 1.0$, the second layer (g)–(l) $I_{2ext} = 2.67$, the third layer (m)–(r) $I_{3ext} = 6.0$, and the coupling intensity between neurons in the same layer is selected at $D = 1$. The snapshots are plotted in color scale. Coupling channels between layers are switched off. (For interpretation of the references to color in this figure legend, the reader is referred to the web version of this article.)

experimental data and the complex nonlinear dynamics in the firing patterns of a sciatic nerve chronic constriction injury model was discussed [9]. *Ibarz et al.* [10] thought that map-based neuron model could also be effective to produce the dynamical properties of neuron. *Brette* [11] considered spiking neuron models defined by a one-dimensional differential equation, and then the implications of these mathematical results in terms of neural coding and spike timing precision were investigated *Ji et al.* [12] reported a piece-wise linear planar neuron model, namely, two-dimensional McKean model with periodic drive, and the bifurcation mechanism for the bursting solution induced by the slowly varying periodic drive was presented. *Yu et al.* [13] investigated the synchronization of neuron population subject to steady DC electric field induced by magnetic stimulation; the effect of steady DC electric field induced by magnetic stimulation on the coherence of an interneuronal network was discussed. *Wang et al.* [14] studied the phase synchronization involving burst synchronization and spike synchronization of two electrically coupled Hindmarsh–Rose neurons, and found that the existence of equilibria can be turned into intersection of two odd functions in a non-delayed system A recurrent loop consisting of a single Hodgkin–Huxley neuron influenced by a chemical excitatory delayed synaptic feedback was considered [15], and it is found that the behavior of the system depends on the duration of the activity of the synapse *Tang et al.* [16] constructed a minimal neuron–astrocyte network model by connecting a neurons chain and an astrocytes chain, and it is found that calcium wave

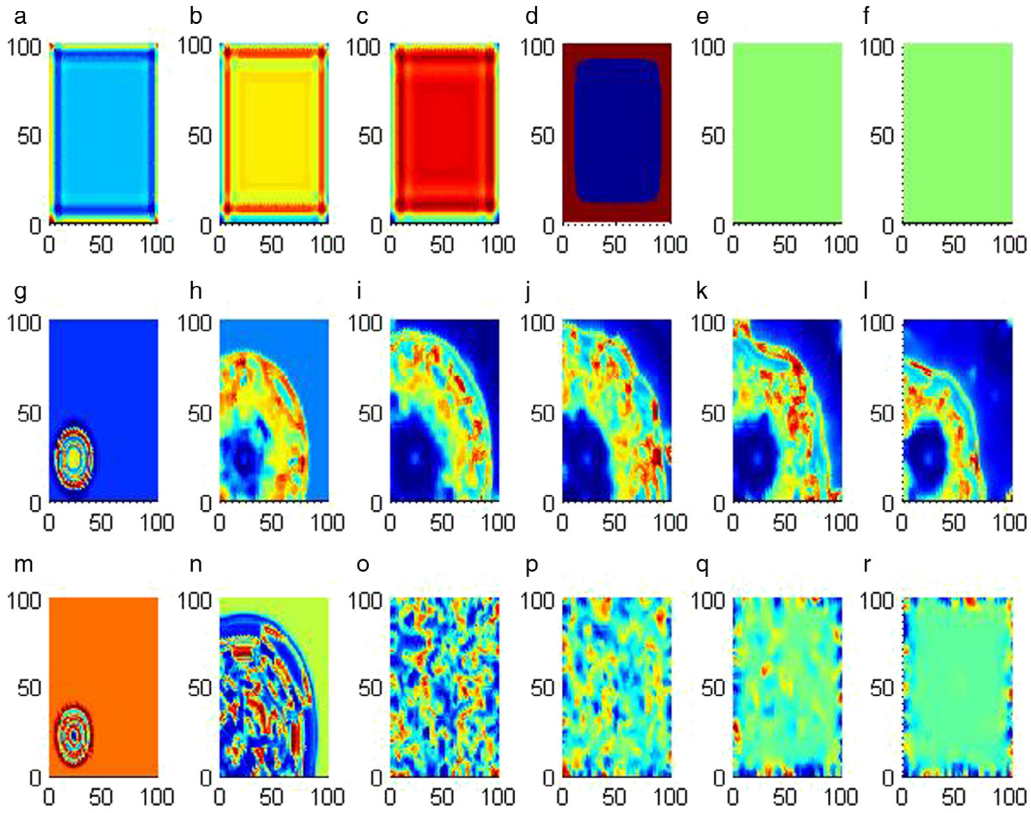

Fig. 3. Developed spatial pattern is plotted for the tri-layer network at $t = 50, 150, 500, 1000, 1500, 2500$ time units. The first layer (a)–(f) is driven by $I_{1ext} = 1.0$, the second layer (g)–(l) $I_{2ext} = 2.67$, the third layer (m)–(r) $I_{3ext} = 6.0$, and the coupling intensity between neurons in the same layer is selected at $D = 1$. Coupling channels between the three layers are switched on at $t = 15$ time units, the coupling intensity between adjacent layers is set as $k = 1.0$ and the coupling is nonreciprocal type as described in Eqs. (2).

propagation in astrocytes determines the propagation of SDs in the connected neurons. Based on these neuronal models, extensive dynamical analysis and control have been carried out for potential applications. For example, *Guo et al.* [17] analyzed the dynamics of network of neuron-coupled astrocyte when autaptic driving is applied. *Wang et al.* [18] explained the formation mechanism of autapse connection to neuron based on a cable neuron model and confirmed that injury in neuron could contribute to the formation of autapse. Similar to the chaotic oscillators, bifurcation parameter in neuronal model plays an important role in selecting modes of electrical activities, and the parameter estimation becomes attractive for further investigation on transition of electrical activities. *Tyukin et al.* [19] considered the problem of how to recover the state and parameter values of typical model neurons, such as Hindmarsh–Rose, FitzHugh–Nagumo, Morris–Lecar, from in-vitro measurements of membrane potentials. *Ozer et al.* [20] investigated the contribution of subthreshold periodic current forcing on synchronization of neuronal spiking activity. *Wang et al.* [21] suggested adaptive synchronization and anti-synchronization can be used to identify the unknown parameters of the neuronal model.

Indeed, some realistic factors should be considered in analyzing the dynamical properties of neuronal activities. For example, noise can change the dynamics of electrical activities synchronization behavior and pattern formation of neurons [22–24]. The electromagnetic induction plays an important role in changing the modes of electric activities [25]; it is found that multiple modes of electrical activities can be detected by adjusting the external electromagnetic radiation on the improved neuron model by mapping the electromagnetic induction with magnetic flux variable [26]. Autapse, which is a specific synapse connected the axon and dendrites of the same neuron via close loop, this type of connection is described by time-delayed feedback on a close loop and this time delay is called as intrinsic response time delay [27–29]. The neuron shows sensitive response to electrical autapse than the chemical autapse [30], and the dynamical properties of electrical activities such as firing pattern of neurons can be adjusted by autaptic inhibition [31,32]. Furthermore, distribution of autapse connection in the network can regulate the collective behaviors of network like a pacemaker [33,34] by generating continuous pulses [35], target waves [36], spiral waves [37], and also can block the wave propagation by generating defects [38] due to negative feedback from autapse driving. Extensive studies confirmed that autapse driving is effective to enhance synchronization of coupled neurons and network [39]. Isolate neuron setting and appropriate dynamical analysis are helpful to understand the mode transition of electrical activities, and also potential mechanism for occurrence of neuronal

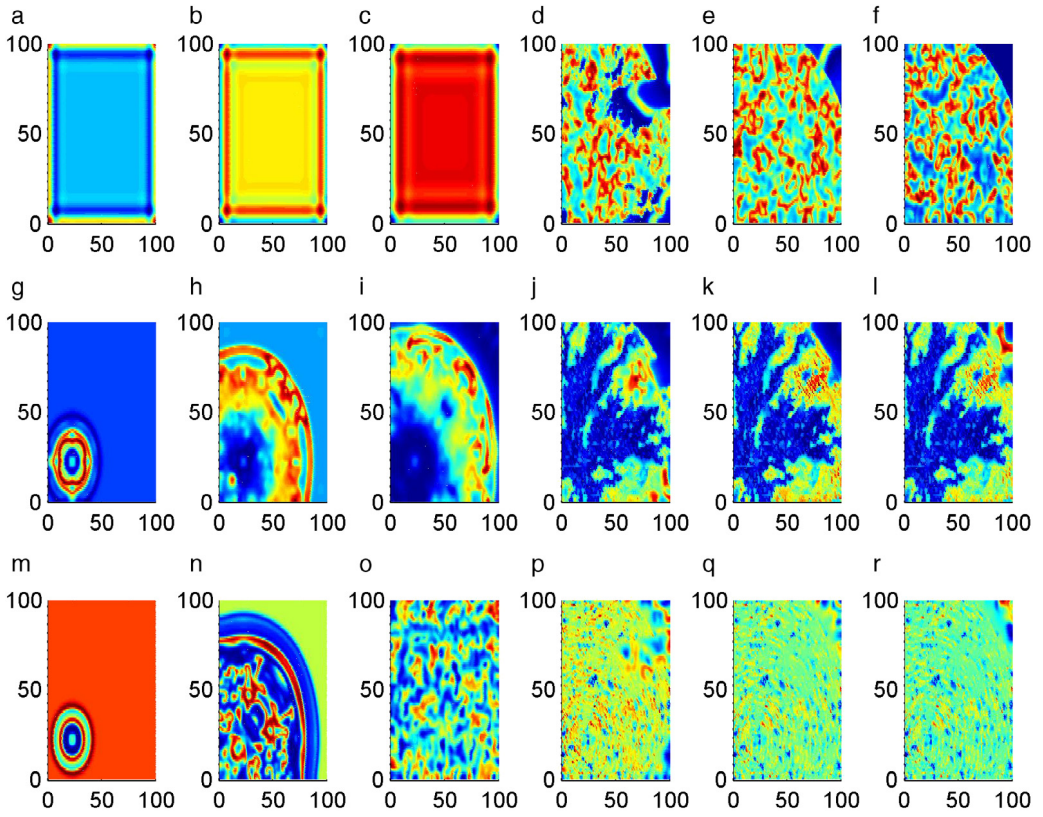

Fig. 4. Developed spatial pattern is plotted for the tri-layer network at $t = 50$, 150, 500, 1000, 1500, 2500 time units. The first layer (a)–(f) is driven by $I_{1ext} = 1.0$, the second layer (g)–(l) $I_{2ext} = 2.67$, the third layer (m)–(r) $I_{3ext} = 6.0$, and the coupling intensity between neurons in the same layer is selected at $D = 1$. Coupling channels between the three layers are switched on at $t = 15$ time units, the coupling intensity between layers is set as $k = 1.0$, and the coupling is nonreciprocal type as described in Eqs. (2). Within the first layer, the bifurcation parameter χ is switched from 1.56 to zero from $t = 500$ time units.

disease. While most of the researchers thought collective behaviors of neurons should be considered on networks under different topological connection and controllable conditions [40–42] For example, Stochastic and coherence resonance in neuronal network [43–46], and pacemaker-guided spatial regularity [47] in excitable media can give important guidance and understanding on self-organization, synchronization [48] in neuronal network in presence of noise, also signal detection [49] as well. On the other hand, the pattern formation of neuronal network could give useful guidance to understand the phase transition and mode changes of electrical activities for a set of large number of neurons. However, most of these works have been carried out on one layer of network even though the neurons are connected in complex type. As a result, *Qin et al.* [50] investigated the synchronization between two-layer network of neurons under cross-coupling between the two layers, and found that synchronization can be enhanced when more neurons took part in the coupling between two layers by generating stable wave source such as target wave or spiral wave (pace maker) in the first layer. Readers can refer to a review [51–53] for the dynamical behavior of neuronal networks and references therein.

In complex biological and ecological systems, multiple layers of network could be used to describe the diversity in neurons so that identical nodes can be collected into the same layer. For example, the cardiac tissue is composed of epimyocardium, myocardial intima and myocardium; as a result, three layers can be reliable to describe the difference between each layer of the media. In the cortex, there are many neurons with diversity in excitability. As a result, excitatory and inhibitory type, excitability diversity should be considered. On the other hand, neurons can be under different modes in electrical activities, waken or asleep, quiescent, spiking, bursting or chaotic states, respectively. Therefore, it is interesting to design such a tri-layer network to detect the diffusive effect on different layers in the network, transition of synchronization and pattern selection of each layer under coupling.

In this paper, a tri-layer neuronal network with excitability diversity in layers is used to study the signal propagation and pattern synchronization between layers by observing the pattern transition of the network. The three layers are coupled monodirectionally (nonreversing type) and only finite channels are used to connect the adjacent layers. The first layer is driven to generate pacemaker-like wave source so that the next two layers can be driven to keep pace with the collective behaviors in the first layer. Furthermore, the collapse [54,55] in the first layer is induced by rapid switch in certain parameter, the transition of pattern in the second and third layer of the network are detected and discussed.

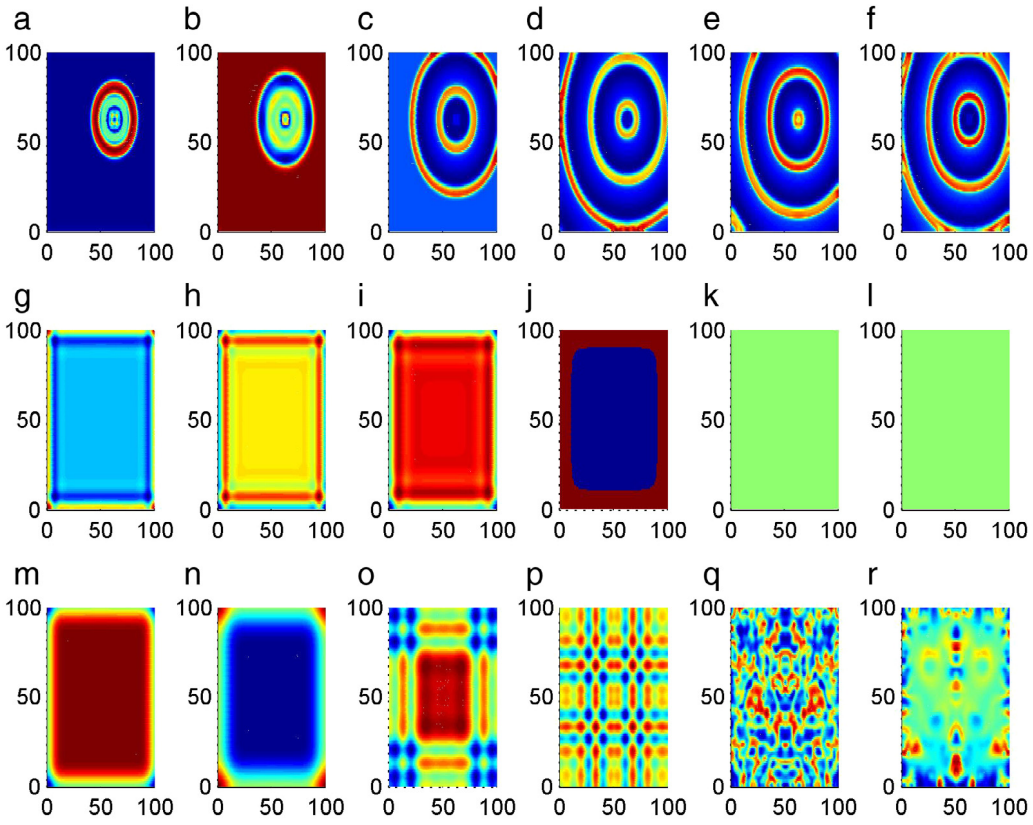

Fig. 5. Developed spatial pattern is plotted for the tri-layer network at $t = 50, 150, 500, 1000, 1500, 2500$ time units. The nodes $(60 \leq i, j \leq 65)$ in first layer (a)–(f) is driven by $I_{1ext} = 2.67$ while other nodes are driven by $I_{1ext} = 1.0$; the second layer (g)–(l) $I_{2ext} = 1.0$; the third layer (m)–(r) $I_{3ext} = 6.0$, and the coupling intensity between neurons in the same layer is selected at $D = 1$. Coupling channels between layers are switched off.

2. Model and scheme

The dynamics of the Hindmarsh–Rose (HR) neuron [56] is described by

$$\begin{cases} \dot{x} = y - ax^3 + bx^2 - z + I_{ext} \\ \dot{y} = c - dx^2 - y \\ \dot{z} = r[s(x + \chi) - z] \end{cases} \tag{1}$$

where the variable x, y, z denotes the membrane potential, slow current for recovery variable and adaption current, respectively. I_{ext} is the external forcing current, and a, b, c, d, r, s, χ are parameters. A quiescent state, spiking, bursting and even chaotic state can be reproduced from this model by changing the external forcing current carefully. For simplicity, the HR neuron is used to describe the local kinetics of each node of the tri-layer network, and network on each layer is coupled with nearest-neighbor connection type (regular network), and the collective dynamical behaviors can be described by

$$\begin{cases} \dot{x}_{1ij} = y_{1ij} - ax_{1ij}^3 + bx_{1ij}^2 - z_{1ij} + I_{1ext} + D(x_{1i-1j} + x_{1i+1j} + x_{1ij-1} + x_{1ij+1} - 4x_{1ij}) \\ \dot{y}_{1ij} = c - dx_{1ij}^2 - y_{1ij} \\ \dot{z}_{1ij} = r[s(x_{1ij} + \chi) - z_{1ij}] \\ \dot{x}_{2ij} = y_{2ij} - ax_{2ij}^3 + bx_{2ij}^2 - z_{2ij} + I_{2ext} + D(x_{2i-1j} + x_{2i+1j} + x_{2ij-1} + x_{2ij+1} - 4x_{2ij}) \\ + k(x_{1ij} - x_{2ij})\delta_{i\alpha}\delta_{j\beta} \\ \dot{y}_{2ij} = c - dx_{2ij}^2 - y_{2ij} \\ \dot{z}_{2ij} = r[s(x_{2ij} + \chi) - z_{2ij}] \\ \dot{x}_{3ij} = y_{3ij} - ax_{3ij}^3 + bx_{3ij}^2 - z_{3ij} + I_{3ext} + D(x_{3i-1j} + x_{3i+1j} + x_{3ij-1} + x_{3ij+1} - 4x_{3ij}) \\ + k(x_{2ij} - x_{3ij})\delta_{i\alpha}\delta_{j\beta} \\ \dot{y}_{3ij} = c - dx_{3ij}^2 - y_{3ij} \\ \dot{z}_{3ij} = r[s(x_{3ij} + \chi) - z_{3ij}] \end{cases} \tag{2}$$

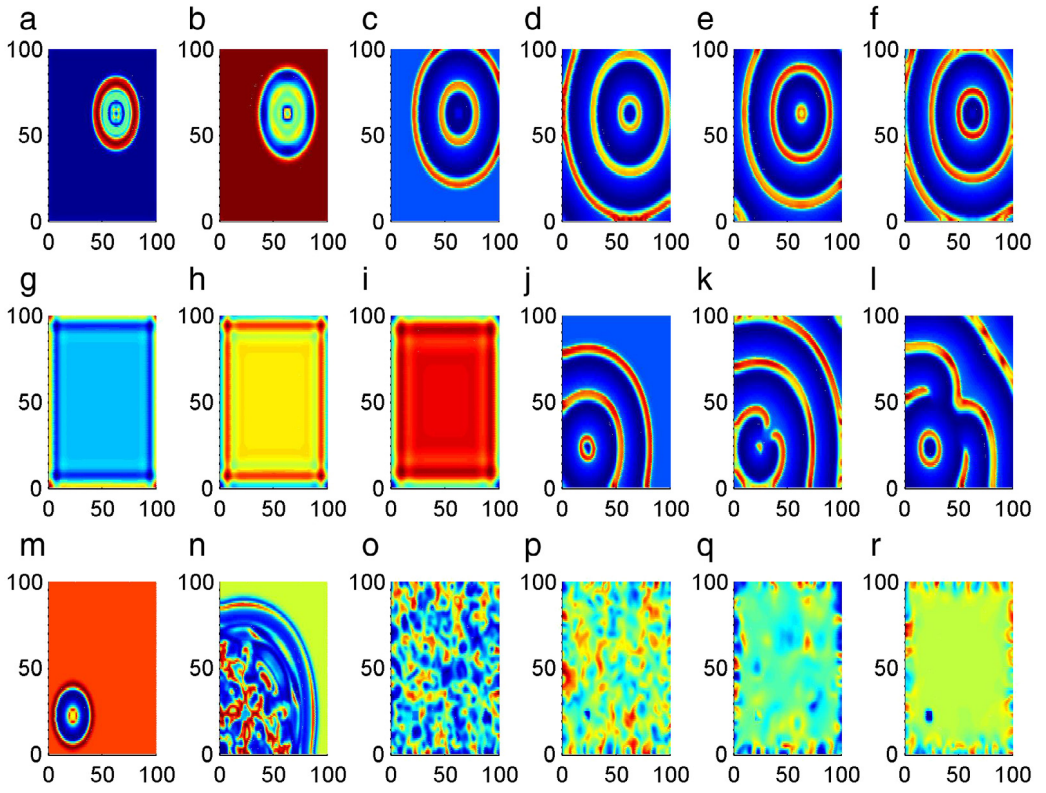

Fig. 6. Developed spatial pattern is plotted for the tri-layer network at $t = 50, 150, 500, 1000, 1500, 2500$ time units. The nodes $(60 \leq i, j \leq 65)$ in first layer (a)–(f) is driven by $I_{1ext} = 2.67$ while other nodes are driven by $I_{1ext} = 1.0$; the second layer (g)–(l) $I_{2ext} = 1.0$; the third layer (m)–(r) $I_{3ext} = 6.0$, and the coupling intensity between neurons in the same layer is selected at $D = 1$. Coupling channels between the three layers are switched on at $t = 15$ time units, the coupling intensity between layers is set as $k = 1.0$, and the coupling is nonreciprocal type as described in Eqs. (2).

where D is the coupling intensity between neurons in the same layer, k is the coupling intensity between adjacent layers. The subscript ij represents the node position in each layer, i, j, α, β,are integers, the function δdefines the number of coupling channels and coupling area as, $\delta_{i\alpha} = 1$ for $\alpha = i$,otherwise, $\delta_{i\alpha} = 0$; $\delta_{j\beta} = 1$ for $\beta = j$,otherwise, $\delta_{j\beta} = 0$. The diagram of the tri-layer network is plotted in Fig. 1.

To discern the phase transition for collective behaviors of neurons on each layer, a statistical factor of synchronization R [36–38] is calculated by using mean field theory, and it reads as follows

$$F = \frac{1}{N^2}\sum_{j=1}^{N}\sum_{i=1}^{N} x_{ij}; \quad R = \frac{\langle F^2\rangle - \langle F\rangle^2}{\frac{1}{N^2}\sum_{j=1}^{N}\sum_{i=1}^{N}\left(\langle x_{ij}^2\rangle - \langle x_{ij}\rangle^2\right)} \tag{3}$$

where x_{ij} is the sampled membrane potential for neuron on node (ij) in the same layer, N^2 neurons are placed on nodes of square array uniformly. The symbol $\langle * \rangle$ represents the average calculating over time (transient period). Perfect synchronization is realized in the network (each layer) at $R \sim 1$ while non-perfect synchronization or desynchronization is found at $R \sim 0$. It is also confirmed that regular spatial pattern can be developed in the network at lower factor of synchronization, while higher factor of synchronization can generate homogeneous state in the network because each neuron can keep pace with the behavior of other neurons. That is to say, complete synchronization in the network of each layer makes the network become homogeneous thus no regular spatial pattern can be formed. To discern the competition and cooperation between layers of the network, each layer is set as different states. Certain parameter is switched from previous value to another value to induce collapse of network, thus the collapse-induced disorder and transition of collective behaviors, synchronization transition of network can be detected. In a realistic network, collapse associated with sudden parameter changes could be diffusive and more nodes are invaded to cause a breakdown in network. For simplicity, the collapse of parameter χ begins from node (52, 32) and its adjacent four nodes, and the parameter $\chi = 1.56$ in the HR neuronal model is switched to $\chi = 0$ at $t = 500$ time units. The outer adjacent neurons are invaded within 1.5 time units until the collapsed area covers more neurons because the collapsed area always is increased in size. Coupling channels between the three layers are switched on at $t = 15$ time units to observe the diffusive effect between layers.

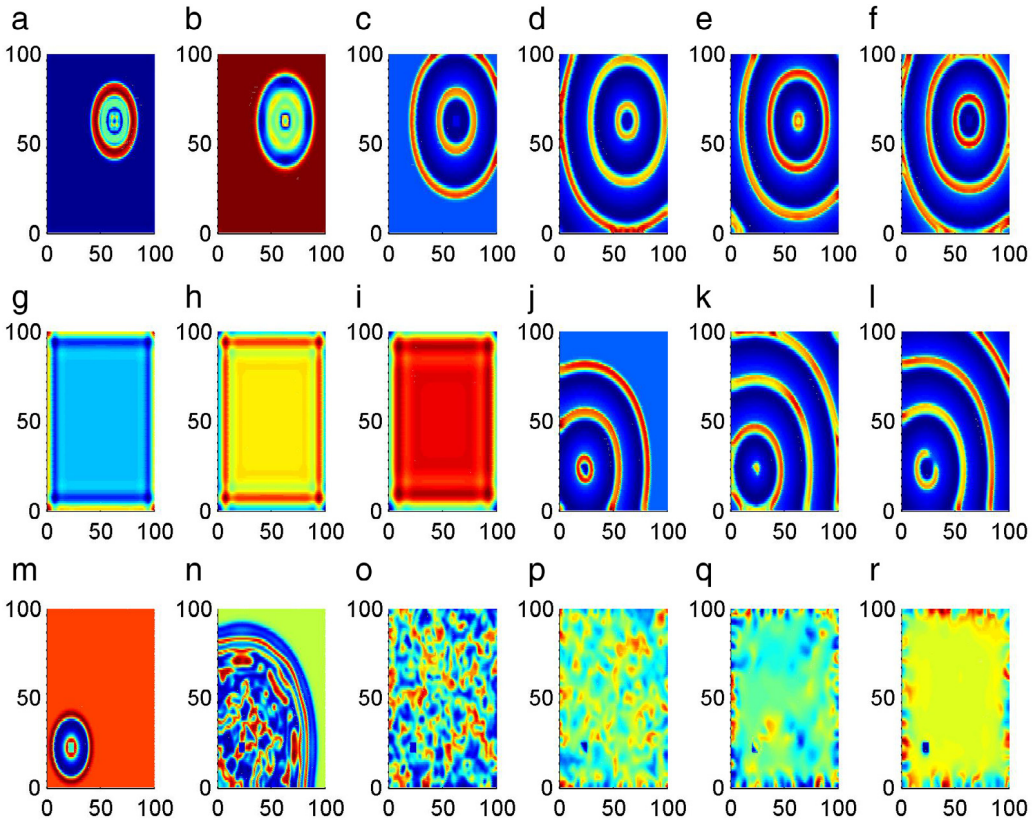

Fig. 7. Developed spatial pattern is plotted for the tri-layer network at $t = 50, 150, 500, 1000, 1500, 2500$ time units. The nodes $(60 \leq i, j \leq 65)$ in first layer (a)–(f) is driven by $I_{1ext} = 2.67$ while other nodes are driven by $I_{1ext} = 1.0$; the second layer (g)–(l) $I_{2ext} = 1.0$; the third layer (m)–(r) $I_{3ext} = 6.0$, and the coupling intensity between neurons in the same layer is selected at $D = 1$. Coupling channels between the three layers are switched on at $t = 15$ time units, the coupling intensity between layers is set as $k = 5.0$, and the coupling is nonreciprocal type as described in Eqs. (2).

3. Numerical results and discussion

In the numerical studies, the Euler forward algorithm is carefully used for calculating the dynamical equations for networks with time step $h = 0.01$. Indeed, fourth order Runge–Kutta algorithm can be used for higher accuracy in numerical studies. In fact, in case of pattern selection and synchronization of multi-layer network or network composed of a large number of nodes, Euler forward algorithm is exact enough to detect the statistical properties and transition of collective behaviors of network. To decrease and shorten the calculating period, we prefer to use the Euler forward algorithm than fourth order Runge–Kutta algorithm by applying appropriate time steps. The network is considered under no-flux boundary condition and all the nodes are selected with the same initial values as (3.0, 0.3, 0.1), 100×100 neurons are placed on the square array in each layer uniformly. In the end, the case that initial values are selected by random value is also discussed. The parameters are selected as $a = 1, b = 1, c = 3, d = 5, r = 0.006, s = 4$, and $\chi = 1.56$. In this section, the first layer is set as quiescent state, target wave controlled state, and then diffusive collapse is considered in the first layer of the network. The transition of spatial patterns in the second and third layer of the network is detected. Finally, the effect of coupling channels is investigated by calculating the factor of synchronization.

Each node of the first layer is driven by same external forcing current as $I_1 = 1.0, I_2 = 2.67$ for second layer and $I_3 = 6.0$ for the third layer of the network. As a result, the first layer can generate quiescent and homogeneous state, the second layer presents bursting and disordered state, while the third layer can find chaotic and disordered state when the coupling channels between layers are cut off and the results are calculated in Fig. 2. The following snapshots are the distribution of variable (membrane potential of neuron) x_{ij}, and the color diversity is generated due to the difference of membrane potentials for neurons.

The results in Fig. 2 found that the developed states of the network depend on the external forcing current and the coupling intensity, thus different spatial states can be formed in each isolate layer. Furthermore, the tri-layer network is activated by switching on the coupling channels between adjacent layers of the network. For simplicity, neurons on the nodes $20 \leq \alpha, \beta \leq 25$ in each layer are connected to the next adjacent layer. The transition of spatial patterns on the network is plotted in Fig. 3.

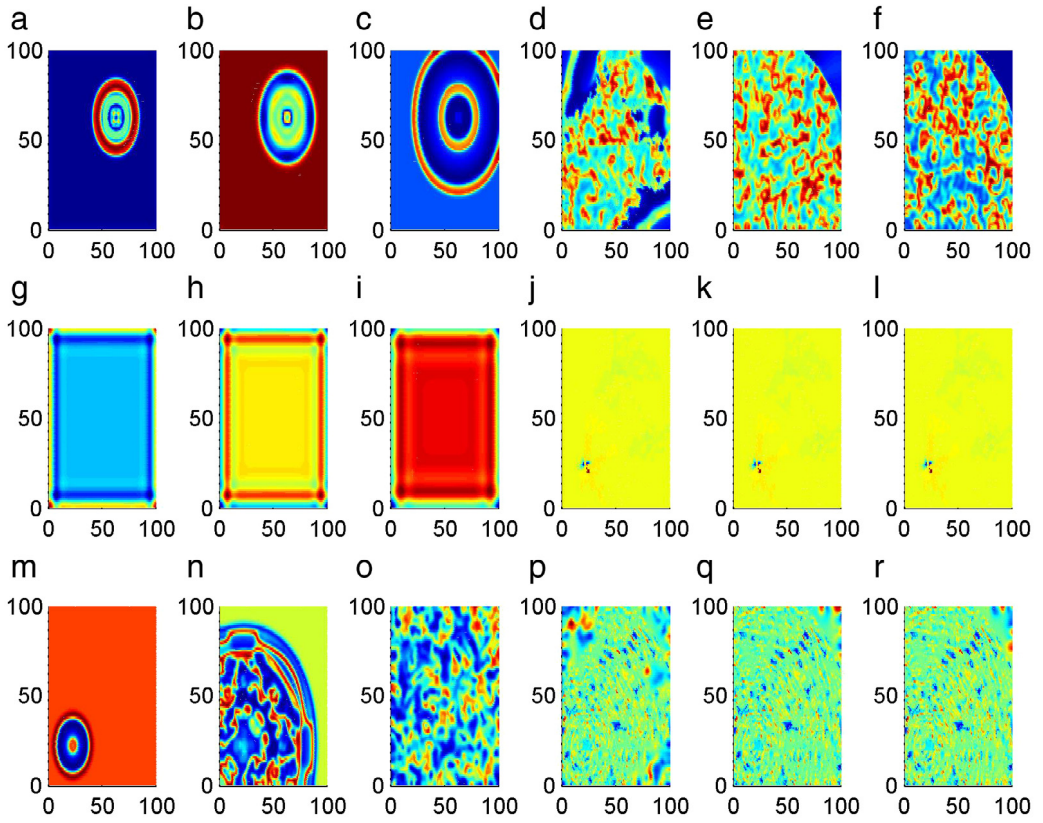

Fig. 8. Developed spatial pattern is plotted for the tri-layer network at $t = 50, 150, 500, 1000, 1500, 2500$ time units. The nodes $(60 \leq i, j \leq 65)$ in first layer (a)–(f) is driven by $I_{1ext} = 2.67$ while other nodes are driven by $I_{1ext} = 1.0$; the second layer (g)–(l) $I_{2ext} = 1.0$, the third layer (m)–(r) $I_{3ext} = 6.0$, and the coupling intensity between neurons in the same layer is selected at $D = 1$. The parameter $\chi = 1.56$ in the HR neuronal model is switched to $\chi = 0$ at $t = 500$ time units. Coupling channels between the three layers are switched on at $t = 15$ time units, the coupling intensity between layers is set as $k = 1.0$, and the coupling is nonreciprocal type as described in Eqs. (2).

It is interesting to find that target like wave is formed in the local area of the second and third layer due to the coupling between layers in the local area. The coupling area in the second layer is driven by quiescent signals from the first layer thus the transient wave front could be suppressed by the bursting states in the second layer even though target-like wave is triggered in the local area connected to the first layer. In fact, for the second and third layer, finite channel connection can input external stimuli with diversity thus target wave can be formed in a local area. However, the emergence of target wave in the local area connected to other layers are suppressed by the wave fronts emitted from other nodes in the same layer, as a result, the third layer is also occupied by disordered state completely. As reported in Refs. [54,55], collapse of network can be induced by rapid shift in parameter, which certain parameter is changed to another value suddenly. The potential mechanism is that switch in parameter value can change the local kinetics of node of the network, and the destruction or invading can be diffused among the network due to continuous coupling between adjacent nodes. It is interesting to investigate the signal propagation between layers in the tri-layer network when parameter collapse occurs in the first layer, which the bifurcation parameter χ is switched from 1.56 to zero (in addition, other values also finds the similar results), and the results are plotted in Fig. 4.

The results in Fig. 4 confirmed that the collapse can be propagated outwardly and can also induce breakdown in the second and third layers of the network. That is, collapse in the above layer can enhance breakdown and disorder in the next layers due to channel coupling between layers. It is interesting to investigate the case whether target wave in the first layer can suppress the disordered states on the second and third layers. For simplicity, forcing current with diversity is imposed on the first layer so that target wave can be developed, e.g. in the local area $60 \leq i, j \leq 65$ the external forcing current $I_{1ext} = 2.67$, the other nodes of the first layer are driven by $I_{1ext} = 1.0$, and the results are plotted in Fig. 5.

It is found that the each layer develops its state under appropriate external forcing current when the coupling channels between layers are shut off. The first layer is occupied by stable target wave when external forcing current with diversity is formed; the second layer keeps quiescent state while the third layer steps into spatiotemporal disorder. Furthermore, the coupling channels are switched on, the propagation of target wave and response of the second and third layer of the network are detected, the results are plotted in Fig. 6.

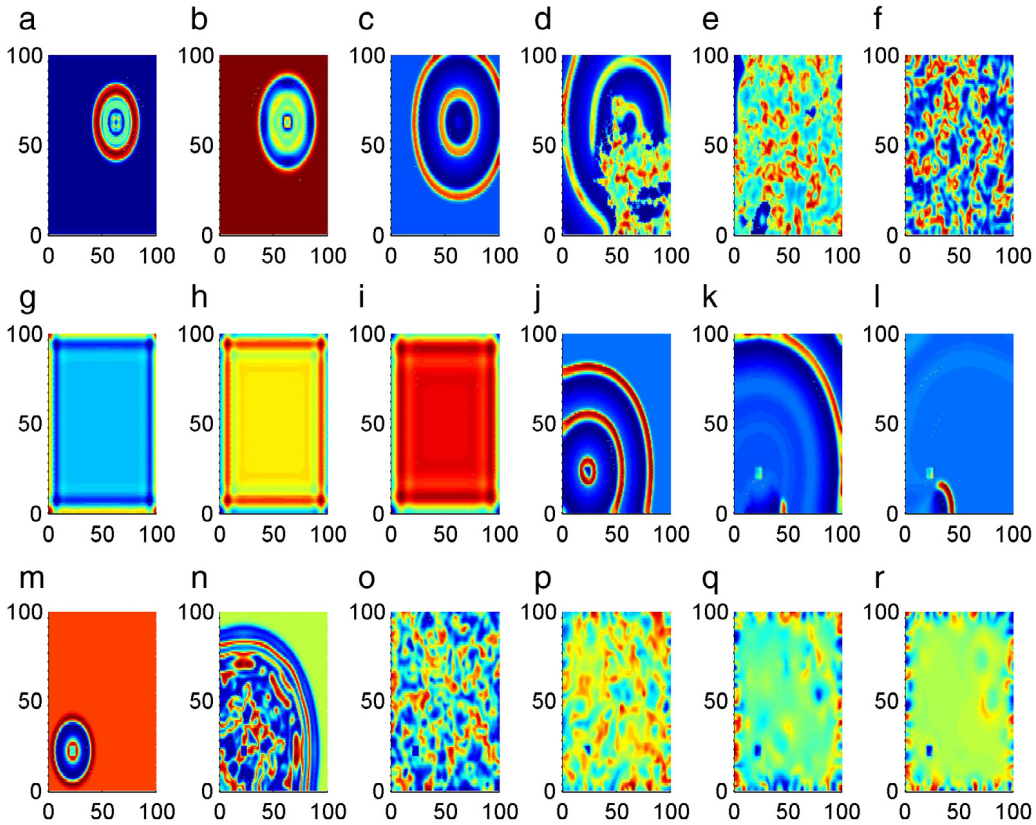

Fig. 9. Developed spatial pattern is plotted for the tri-layer network at $t = 50, 150, 500, 1000, 1500, 2500$ time units. The nodes $(60 \leq i, j \leq 65)$ in first layer (a)–(f) is driven by $I_{1ext} = 2.67$ while other nodes are driven by $I_{1ext} = 1.0$; the second layer (g)–(l) $I_{2ext} = 1.0$,; the third layer (m)–(r) $I_{3ext} = 6.0$, and the coupling intensity between neurons in the same layer is selected at $D = 1$. The parameter $\chi = 1.56$ in the HR neuronal model is switched to $\chi = 0$ at $t = 500$ time units. Coupling channels between the three layers are switched on at $t = 15$ time units, the coupling intensity between layers is set as $k = 5.0$, and the coupling is nonreciprocal type as described in Eqs. (2).

The development of spatial patterns found that target wave kept alive and transient target wave is also developed in a local area of the second layer due to driving from the first layer, and the unstable target wave close to the coupling area in the second layer finally developed into spiral segments for growing up spiral wave. Furthermore, breakup of the target wave in the second layer generates continuous disturbance on the third layer via channel coupling, as a result, the third layer became disordered completely. It is interesting to explore this case when the coupling intensity between layers is increased, and the results are plotted in Fig. 7.

It is found that target wave can also be developed in the second layer with increasing the coupling intensity between the layers; however, wave front of the third layer is suppressed by the spatiotemporal chaos and the target like wave encounters breakup to generate more segments. That is to say, the developed target wave cannot be effective to induce stable target wave in the third layer via finite channel coupling between the second and third layer. Furthermore, the coupling intensity between the second and third layer is increased together with the increasing the number of coupling channels, it is confirmed that target wave can also be developed. It is known that spiral wave can be formed by breaking target wave or plane wave in the media, and the self-sustained spiral wave can regulate the collective behaviors of network. Therefore, collapse in parameter is considered in the first layer by switching the parameter from $\chi = 1.56$ to $\chi = 0$ at $t = 500$ time units, and the results are shown in Fig. 8.

The developed target wave in first layer is broken due to parameter collapse, and the diffusive collapse in parameter destroys the target wave completely. Furthermore, the target wave in the second layer was also broken into segments and spiral waves are formed. However, the third layer cannot support spiral wave nor target wave even channel coupling keep active. Extensive numerical results are carried out by increasing the intensity of channel coupling $k = 5$, and the results are shown in Fig. 9.

Similar to the case in Fig. 8, the first layer is occupied segments developed from broken target wave due to diffusive collapse in parameter, the second layer can form spirals due to breakup of target wave. The third layer also finds spatiotemporal chaos when the disordered signals from the second layer are imposed on the third layer of the network.

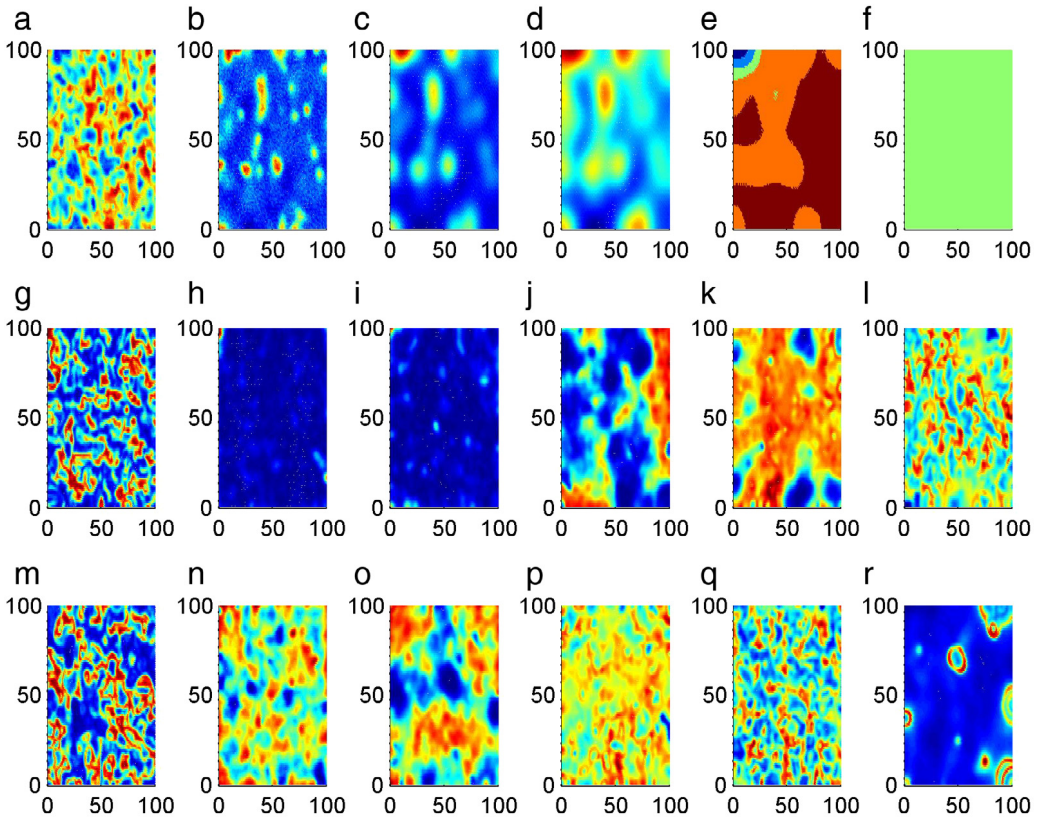

Fig. 10. Developed spatial pattern is plotted for the tri-layer network at $t = 50, 150, 500, 1000, 1500, 2500$ time units. The first layer (a)–(f) is driven by $I_{1ext} = 1.0$, the second layer (g)–(l) $I_{2ext} = 2.67$, the third layer (m)–(r) $I_{3ext=}6.0$, and the coupling intensity between neurons in the same layer is selected at $D = 1$. The snapshots are plotted in color scale. Coupling channels between layers are switched off and random values are used for initials setting. (For interpretation of the references to color in this figure legend, the reader is referred to the web version of this article.)

As mentioned above, all the nodes in each layer are set with the same initial values. It is interesting to discuss the case when initials are selected with random values $(-0.1, 0.1)$, the pattern formation and synchronization between layers are investigated in the same way, the results are shown in Fig. 10 when channels between layers are switched off.

It is found that the developed state in each layer is different from the next layer when each layer is imposed on different external forcing currents. As a result, the first layer is developed into homogeneous state and each neuron become quiescent completely. The second and third layer of the network become disordered states when larger external forcing current is imposed on each node, and coupling in each layer can enhance the oscillating behaviors. In the following, the coupling channels are switched on, and the synchronization, pattern formation is investigated in Fig. 11.

Compared the results in Fig. 11 with the results in Fig. 9, the disordered states in the second layer is suppressed when sampled signals are input into the layer via coupling channels, and the third layer is also suppressed as well. Extensive numerical results confirmed that the second and third layer will keep pace with the states in the first layer when the coupling intensity in channels between layers is increased. Furthermore, we also investigated the case when parameter shift-induced collapse is considered, and the results are plotted in Fig. 12.

It is found that collapse in the first layer can induce disordered states, as a result, the sampled signals are imposed on the second layer and this type of disturbance can enhance the disorder in the second layer, and also the third layer as well. By further increasing the coupling intensity between layers, the collective behaviors and spatial pattern in the next layer is controlled by the sampled signals from the previous (above) layer.

Indeed, the synchronization between layers of the network is also dependent on the channel number involved with coupling between layers when the coupling intensity is fixed. Therefore, it is important to investigate the pattern formation in the tri-layer network when different numbers of coupling channels are switched on between the layers. The first, second and third layer is reset as ordered state (e.g. target wave), quiescent state and chaotic state, which can be realized by applying different external stimuli and the developed state could be independent of the setting of initial values (random or identical initials). The collapse in parameter begins from the first layer, the number for coupling between layers is selected by $n*n = 1$, 4, 9, 16, 25, for example, $n * n = 25$ means that nodes in a square array with 5×5 nodes are connected to 5×5 nodes in the next layer of the network, $n * n = 1$ means that a single channel keeps open between the adjacent layers. The factor of synchronization is calculated under different numbers of coupling channels, and the results are shown in Fig. 13.

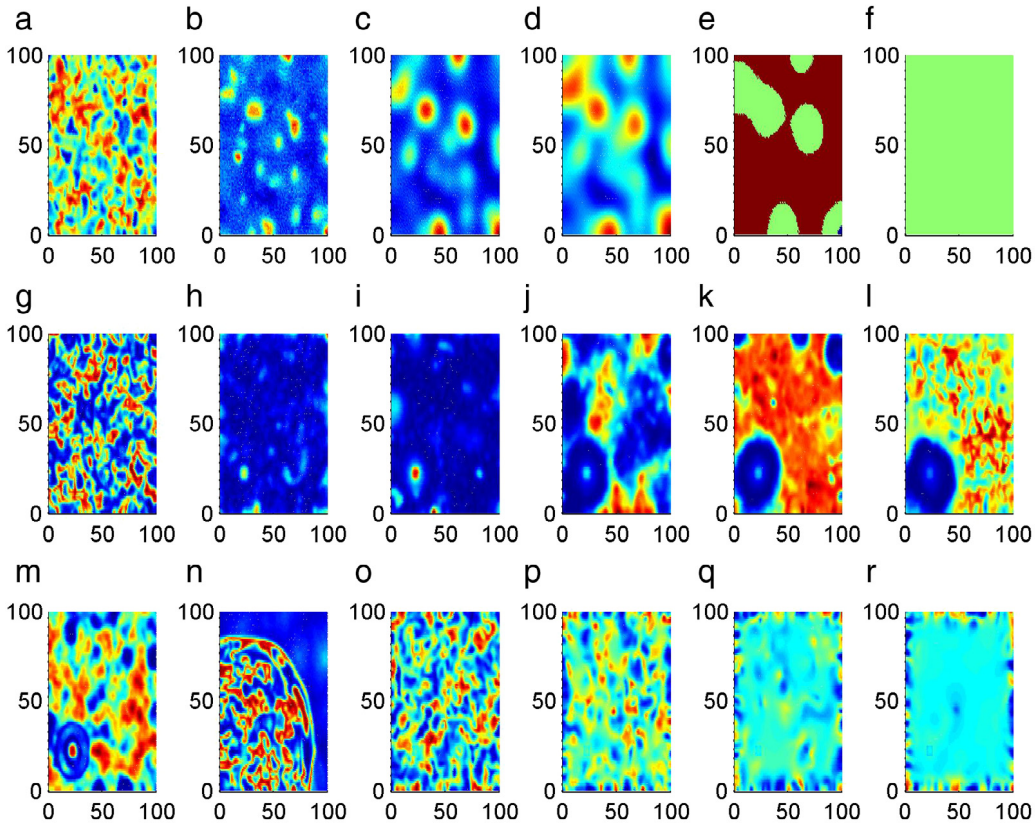

Fig. 11. Developed spatial pattern is plotted for the tri-layer network at $t = 50, 150, 500, 1000, 1500, 2500$ time units. The first layer (a)–(f) is driven by $I_{1ext} = 1.0$, the second layer (g)–(l) $I_{2ext} = 2.67$, the third layer (m)–(r) $I_{3ext=}6.0$, and the coupling intensity between neurons in the same layer is selected at $D = 1$. Coupling channels between the three layers are switched on at $t = 15$ time units, the coupling intensity between layers is set as $k = 1.0$ and the coupling is nonreciprocal type as described in Eqs. (2). Random values are used for initials setting.

As mentioned in the previous works, smaller factor of synchronization is often associated with regular spatial distribution. For example, the network is occupied by a target wave or spiral wave which regulates the network as a pacemaker, while spiral pattern is destroyed and synchronization is enhanced under higher factor of synchronization. The factor of synchronization for the third layer confirmed that phase transition occurs when external forcing is imposed on the third layer and number of coupling channels is increased. The factor of synchronization for the first layer shows slight a change when the target wave is invaded (or destroyed) by diffusive collapse in parameter, thus the regular spatial distribution is suppressed. The factor of synchronization for the second layer keeps lower value because target like wave can be developed due to driving from the first layer via finite channels. We also investigated the case that diffusive collapse occurred in the second layer, while the first layer, the third layer is driven by the second layer as well, the results are plotted in Fig. 14.

It is found that the driving layer (second layer) holds higher factor of synchronization and presents slight changes even the number of coupling channels is increased, the driven layers (the first and third layer) gave different responses when more coupling channels are switched on. The first layer still holds smaller factor of synchronization because the initial quiescent state is helpful to support ordered wave, while the third layer under initial chaotic state can suppress the external forcing from the driving (second) layer via finite coupling channels. Furthermore, coupling channels (4×4) connected to the first and third layer are switched to different areas, which is similar to the cross coupling between two-layer network in Ref. [50], it is found that the synchronization factors for each layer keep close to certain values and also the spatial distribution shows slight difference. It indicates that the pattern formation on each layer depends on the initial selection [57] (quiescent, spiking, or chaotic state, which can be developed from arbitrary initial values by applying appropriate external forcing current), and also the number of coupling channels than the position selection.

Finally, we have to investigate the case that each layer is driven by the next layer, for example, the second layer is driven by the first layer, the third layer is driven by the second layer, the first layer is driven by the third layer. The initial state(developed from arbitrary initial values) for the first layer is selected by quiescent state and diffusive collapse also propagates from the first layer, the second layer is set as bursting initial states, the third layer is under chaotic initial states, the distribution for factors of synchronization is calculated in Fig. 15.

The results in Fig. 15 confirmed that the developed states mainly depend on the initial state (not initial value) for each layer, which is controlled by the external forcing current. The first layer propagates the diffusive collapse in parameter and

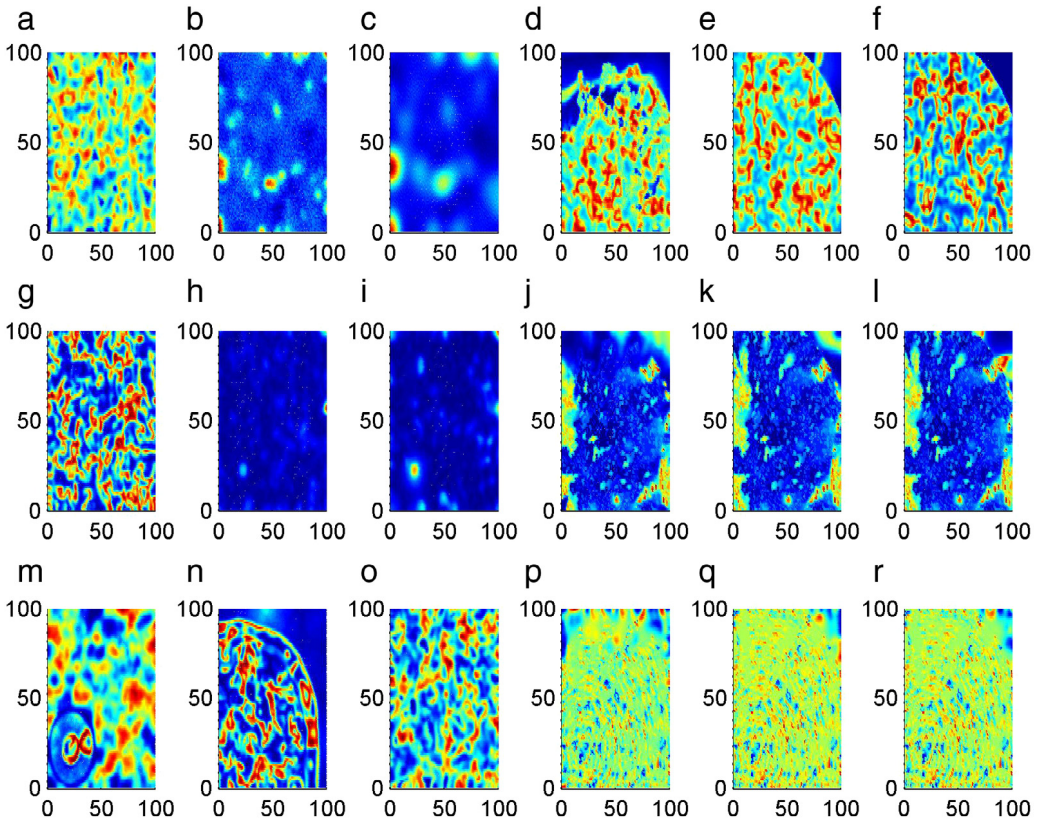

Fig. 12. Developed spatial pattern is plotted for the tri-layer network at $t = 50, 150, 500, 1000, 1500, 2500$ time units. The first layer (a)–(f) is driven by $I_{1ext} = 1.0$, the second layer (g)–(l) $I_{2ext} = 2.67$, the third layer (m)–(r) $I_{3ext} = 6.0$, and the coupling intensity between neurons in the same layer is selected at $D = 1$. Coupling channels between the adjacent layers are switched on at $t = 15$ time units, the coupling intensity between layers is set as $k = 1.0$, and the coupling is nonreciprocal type as described in Eqs. (2). Within the first layer, the bifurcation parameter χ is switched from 1.56 to zero from $t = 500$ time units. Random values are used for initials setting.

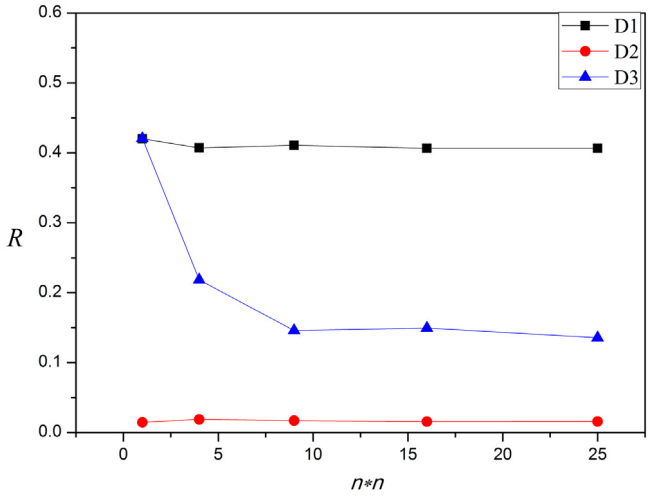

Fig. 13. Distribution for factor of synchronization is calculated by changing the number of coupling channels. The initial state (developed from appropriate value and external forcing current) is selected by target wave (ordered state), quiescent state and chaotic state, respectively. Diffusive collapse in parameter occurs in the first layer. Coupling intensity between layers is selected by $k = 1$. The three lines in color describe the distribution for synchronization factors in different layers. (For interpretation of the references to color in this figure legend, the reader is referred to the web version of this article.)

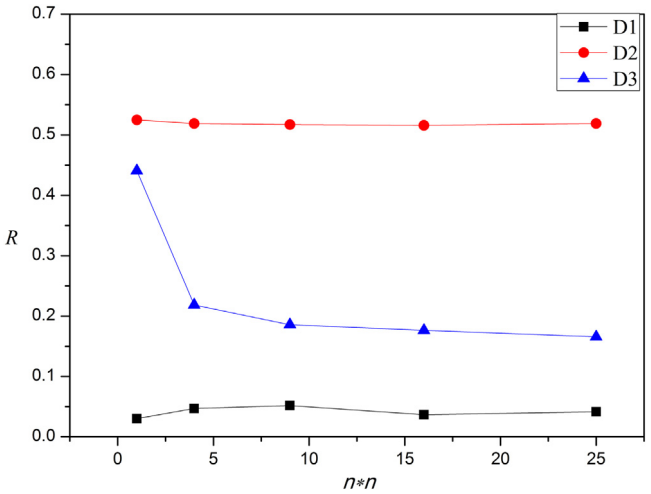

Fig. 14. Distribution for factor of synchronization is calculated by changing the number for coupling channels. The initial state (developed from appropriate value and external forcing current) is selected by target wave (ordered state), quiescent state and chaotic state, respectively. Diffusive collapse in parameter occurs in the second layer and sampled signals are used to drive the first and the third layer via channel coupling. Coupling intensity between layers is selected by $k = 1$. The three lines in color describe the distribution for synchronization factors in different layers. (For interpretation of the references to color in this figure legend, the reader is referred to the web version of this article.)

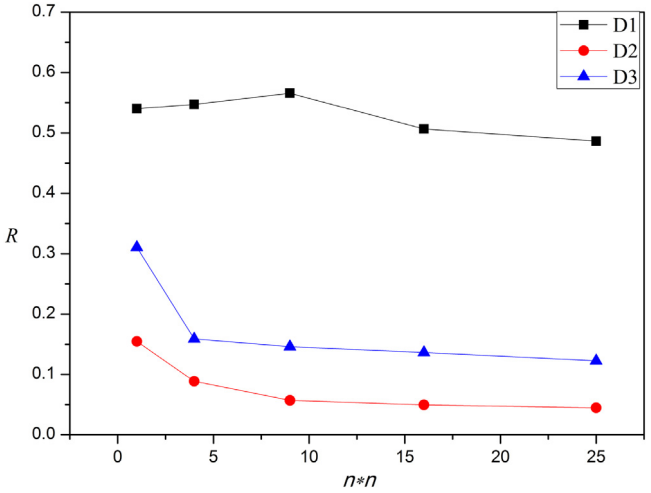

Fig. 15. Distribution for factor of synchronization is calculated by changing the number of coupling channels. The initial state (developed from arbitrary initial values by applying appropriate external forcing current) is selected as quiescent state, bursting and chaotic state, respectively. Diffusive collapse in parameter occurs in the first layer, and coupling intensity between layers is selected by $k = 1$. The three lines in color describe the distribution for synchronization factors in different layers.

the spatial distribution is destroyed. With increasing the number of coupling channels, smaller factor of synchronization is approached in the second and third layer of the network and regular spatial patterns could be formed. For isolate one layer network, spiral wave and target wave can be developed to suppress the spatiotemporal chaos or disordered state. However, the pattern synchronization among layers of multi-layer network becomes difficult, as a result, larger coupling intensity of coupling channels and sufficient coupling channels should be switched on so that different layers can exchange signals and keep pace with each other, in this way, synchronization can be approached.

4. Conclusions

The Hindmarsh–Rose neuron is used to describe the local kinetics of nodes in a multi-layer neuronal network. The network composed of three layers and the adjacent layers are connected with finite coupling channels. In this way, neurons with the same excitability can be included into the same layer while the realistic never system with excitability diversity can be described by a multi-layer network. By imposing appropriate external forcing current, the three different layers can

be kept under quiescent, spiking, bursting, and even chaotic state for each node, and different spatial distributions can be formed. In the case of unidirectional coupling, the second layer can synchronize the first layer and form target wave or spiral wave, while the third layer is often suppressed by disordered state because the developed target wave is neither stable nor powerful. Furthermore, diffusive collapse in parameter realized by sudden switch in certain parameter is considered in the network. It is found that the diffusive collapse in the first layer can be propagated to the next layer even the coupling channel is under finite number. Furthermore, it is found that the synchronization pattern between different layers also depends on the number of coupling channels connected to the adjacent layers. Our results could give possible guidance to understand the signal propagation between different function regions and mode selection to different external stimulus.

Acknowledgment

This project is partially supported by the National Natural Science Foundation of China under Grant Nos. 11365014, 11372122, 11672122.

References

[1] A.L. Hodgkin, A.F. Huxley, A quantitative description of membrane current and its application to conduction and excitation in nerve, J. Physiol. 117 (1952) 500–544.
[2] E.M. Izhikevich, Which model to use for cortical spiking neurons? IEEE Trans. Neural Netw. 15 (2004) 1063–1070.
[3] J.L. Hindmarsh, R.M. Rose, A model of the nerve impulse using two first-order differential equations, Nature 296 (1982) 162–164.
[4] C.M. Liu, X.L. Liu, S.Q. Liu, Bifurcation analysis of a Morris–Lecar neuron model, Biol. Cybernet. 108 (1) (2014) 75–84.
[5] A.V.M. Herz, T. Gollisch, C.K. Machens, et al., Modeling single-neuron dynamics and computations: a balance of detail and abstraction, Science 314 (2006) 80–85.
[6] L. Benuskova, N. Kasabov, Modeling brain dynamics using computational neurogenetic approach, Cogn. Neurodyn. 2 (2008) 319.
[7] V. Volman, M. Bazhenov, T.J. Sejnowski, Computational models of neuron-astrocyte interaction in epilepsy, Front. Comput. Neurosci. 6 (2012) 58.
[8] H.G. Gu, B.B. Pan, G.R. Chen, Biological experimental demonstration of bifurcations from bursting to spiking predicted by theoretical models, Nonlinear Dynam. 78 (2014) 391–407.
[9] H.G. Gu, B.B. Pan, A four-dimensional neuronal model to describe the complex nonlinear dynamics observed in the firing patterns of a sciatic nerve chronic constriction injury model, Nonlinear Dynam. 81 (2015) 2107–2126.
[10] B. Ibarz, J.M. Casado, M.A.F. Sanjuán, Map-based models in neuronal dynamics, Phys. Rep. 501 (2011) 1–74.
[11] R. Brette, The Cauchy problem for one-dimensional spiking neuron models, Cogn. Neurodyn. 2 (2008) 21–27.
[12] Y. Ji, X.F. Zhang, M.J. Liang, et al., Dynamical analysis of periodic bursting in piece-wise linear planar neuron model, Cogn. Neurodyn. 9 (6) (2005) 573–579.
[13] K. Yu, J. Wang, B. Deng, et al., Synchronization of neuron population subject to steady DC electric field induced by magnetic stimulation, Cogn. Neurodyn. 7 (2013) 237–252.
[14] H.X. Wang, Q.Y. Wang, Q.S. Lu, et al., Equilibrium analysis and phase synchronization of two coupled HR neurons with gap junction, Cogn. Neurodyn. 7 (2013) 121–131.
[15] M. Hshemi, A. Valizadeh, Y. Azizi, Effect of duration of synaptic activity on spike rate of a Hodgkin–Huxley neuron with delayed feedback, Phys. Rev. E 85 (2012) 021917.
[16] J. Tang, J. Zhang, J. Ma, et al., Astrocyte calcium wave induces seizure-like behavior in neuron network, Sci. China Technol. Sci. 60 (7) (2017) 1011–1018.
[17] S.L. Guo, J. Tang, J. Ma, et al., Autaptic modulation of electrical activity in a network of neuron-coupled astrocyte, Complexity 2017 (2017) 4631602.
[18] C.N. Wang, S.L. Guo, Y. Xu, et al., Formation of autapse connected to neuron and its biological function, Complexity 2017 (2017) 5436737.
[19] I. Tyukin, E. Steur, H. Nijmeijer, et al., State and parameter estimation for canonic models of neural oscillators, Int. J. Neural Syst. 20 (2010) 193.
[20] M. Ozer, M. Uzuntarla, S.N. Agaoglu, Effect of the subthreshold periodic current forcing on the regularity and the synchronization of neuronal spiking activity, Phys. Lett. A 360 (1) (2006) 135–140.
[21] C.N. Wang, Y.J. He, J. Ma, et al., Parameters estimation, mixed synchronization, and antisynchronization in chaotic systems, Complexity 20 (1) (2014) 64–73.
[22] M. Ozer, N.H. Ekmekci, Effect of channel noise on the time-course of recovery from inactivation of sodium channels, Phys. Lett. A 338 (2005) 150–154.
[23] S.Y. Kim, W. Lim, Noise-induced burst and spike synchronizations in an inhibitory small-world network of subthreshold bursting neurons, Cogn. Neurodyn. 9 (2015) 179–200.
[24] M. Perc, Thoughts out of noise, European J. Phys. 27 (2006) 451–460.
[25] M. Lv, C.N. Wang, G.D. Ren, et al., Model of electrical activity in a neuron under magnetic flow effect, Nonlinear Dynam. 85 (2016) 1479–1490.
[26] M. Lv, J. Ma, Multiple modes of electrical activities in a new neuron model under electromagnetic radiation, Neurocomputing 205 (2016) 375–381.
[27] J.M. Bekkers, Synaptic transmission: functional autapses in the cortex, Curr. Biol. 13 (2003) R433–R435.
[28] C.S. Herrmann, A. Klaus, Autapse turns neuron into oscillator, Int. J. Bifurcation Chaos 14 (2004) 623–633.
[29] H.T. Wang, J. Ma, Y.L. Chen, Y. Chen, Effect of an autapse on the firing pattern transition in a bursting neuron, Commun. Nonlinear Sci. Numer. Simul. 19 (2014) 3242–3254.
[30] X.L. Song, C.N. Wang, J. Ma, et al., Transition of electric activity of neurons induced by chemical and electric autapses, Sci. China Technol. Sci. 58 (2015) 1007–1014.
[31] D.Q. Guo, M.M. Chen, M. Perc, et al., Firing regulation of fast-spiking interneurons by autaptic inhibition, Europhys. Lett. 114 (2016) 30001.
[32] D.Q. Guo, S.D. Wu, M.M. Chen, et al., Regulation of irregular neuronal firing by autaptic transmission, Sci. Rep. 6 (2016) 26096.
[33] E. Yilmaz, V. Baysal, M. Perc, et al., Enhancement of pacemaker induced stochastic resonance by an autapse in a scale-free neuronal network, Sci. China Technol. Sci. 59 (2016) 364–370.
[34] E. Yilmaz, V. Baysal, M. Ozer, et al., Autaptic pacemaker mediated propagation of weak rhythmic activity across small-world neuronal networks, Physica A 444 (2016) 538–546.
[35] H.X. Qin, J. Ma, W.Y. Jin, et al., Dynamics of electrical activities in neuron and neurons of network induced by autapses, Sci. China Technol. Sci. 57 (2014) 936–946.
[36] H.X. Qin, J. Ma, C.N. Wang, et al., Autapse-induced target wave, spiral wave in regular network of neurons, Sci. China Phys. Mech. Astron. 57 (2014) 1918–1926.
[37] J. Ma, H.X. Qin, X.L. Song, et al., Pattern selection in neuronal network driven by electric autapses with diversity in time delays, Internat. J. Modern Phys. B 29 (2015) 1450239.

[38] H.X. Qin, Y. Wu, C.N. Wang, et al., Emitting waves from defects in network with autapses, Commun. Nonlinear Sci. Numer. Simul. 23 (2015) 164–174.
[39] J. Ma, X.L. Song, W.Y. Jin, et al., Autapse-induced synchronization in a coupled neuronal network, Chaos Solitons Fractals 80 (2015) 31–38.
[40] V. Volman, M. Perc, M. Bazhenov, Gap junctions and epileptic seizures–two sides of the same coin? PLoS One 6 (2011) e20572.
[41] P. Suffczynski, S. Kalitzina, F.H.L. Da Silva, Dynamics of non-convulsive epileptic phenomena modeled by a bistable neuronal network, Neuroscience 126 (2004) 467–484.
[42] S. Cullheim, S. Thams, The microglial networks of the brain and their role in neuronal network plasticity after lesion, Brain Res. Rev. 55 (2007) 89–96.
[43] M. Ozer, M. Uzuntarla, T. Kayikcioglu, L.J. Graham, Collective temporal coherence for subthreshold signal encoding on a stochastic small-world Hodgkin–Huxley neuronal network, Phys. Lett. A 372 (43) (2008) 6498–6503.
[44] M. Ozer, M. Perc, M. Uzuntarla, Stochastic resonance on Newman-Watts networks of Hodgkin–Huxley neurons with local periodic driving, Phys. Lett. A 373 (10) (2009) 964–968.
[45] M. Uzuntarla, E. Yilmaz, A. Wagemakers, et al., Vibrational resonance in a heterogeneous Scale Free network of neurons, Commun. Nonlinear Sci. Numer. Simul. 22 (1–3) (2015) 367–374.
[46] M. Perc, Stochastic resonance on excitable small-world networks via a pacemaker, Phys. Rev. E 76 (2007) 066203.
[47] M. Perc, Pacemaker-guided noise-induced spatial periodicity in excitable media, Physica D 238 (2009) 506–515.
[48] D. Guo, Q. Wang, M. Perc, Complex synchronous behavior in interneuronal networks with delayed inhibitory and fast electrical synapses, Phys. Rev. E 85 (2012) 061905.
[49] M. Ozer, M. Perc, M. Uzuntarla, et al., Weak signal propagation through noisy feedforward neuronal networks, NeuroReport 21 (5) (2010) 338–343.
[50] H.X. Qin, J. Ma, W.Y. Jin, et al., Dislocation coupling-induced transition of synchronization in two-layer neuronal networks, Commun. Theor. Phys. 62 (5) (2014) 755–767.
[51] J. Ma, J. Tang, A review for dynamics of collective behaviors of network of neurons, Sci. China Technol. Sci. 58 (2015) 2038–2045.
[52] J. Ma, J. Xu, An introduction and guidance for neurodynamics, Sci. Bull. 60 (2015) 1969–1971.
[53] J. Ma, J. Tang, A review for dynamics in neuron and neuronal network, Nonlinear Dynam. 89 (2017) 1569–1578.
[54] X.L. Song, C.N. Wang, J. Ma, et al., Collapse of ordered spatial pattern in neuronal network, Physica A 451 (2016) 95–112.
[55] J. Ma, Y. Xu, G.D. Ren, et al., Prediction for breakup of spiral wave in a regular neuronal network, Nonlinear Dynam. 84 (2016) 497–509.
[56] J.L. Hindmarsh, R.M. Rose, A model of neuronal bursting using three coupled first-order differential equations, Proc. R. Soc. Lond. Ser. B 221 (1984) 87–102.
[57] J. Ma, Y. Xu, C.N. Wang, et al., Pattern selection and self-organization induced by random boundary initial values in a neuronal network, Physica A 461 (2016) 586–594.